Sound Generation Due to a Spinning Vortex Pair Near the Flat Wall

Sam-Ok Koo*, Ki-Wahn Ryu† and Duck-Joo Lee‡

평면 벽 근처에서 회전하는 와류쌍에 의한 음향발생

구삼옥 유기완 이덕주

벽면 근처에 가까이 위치하는 회전와류쌍을 음원으로 갖는 비정상 유동장에서 벽면이 음장에 미치는 효과를 알아보기 위해 이차원 음장 수치해석을 시도하였다. 비압축성 유동장에 대한 비정상 수력정보를 기반으로 오일러식에서 교란 압축성 소음항을 도출하였다. 원거리 자유경계면은 비반사 경계조건을 이용하였으며, 벽면에서는 벽면 효과를 음향장에 고려하였다. 자유흐름장에 놓인 와류쌍이 대칭인 나선팔을 갖는 반면에, 벽면이 있는 경우엔 음파가 전달되는 경로를 따라 방향성이 존재함을 알 수 있었다. 본 연구를 통하여 벽면이 존재하는 경우에 비정상 수력정보를 이용하여 근거리와 원거리 음장을 동시에 수행할 수 있음을 알아내었다.

Key Words : CAA (전산공력음향학), Spinning Vortex (회전와류), Wall Effect (벽 효과), Non-reflecting BC (비반사 경계조건), Hydrodynamic Density (수력밀도), Near Field (근거리), Far Field (원거리)

Nomenclature

$\mathbf{A}, \mathbf{B}$ = Jacobian matrices
a_0 = ambient speed of sound
$\mathbf{E}, \mathbf{F}$ = flux vectors in the ξ and η directions
h = vertical distance from the wall
J = Jacobian metrics
J_2 = Bessel function of the 1^{st} kind of order 2
k = wave number $(2\omega/a_0)$
M_r = rotating Mach number
p = hydrodynamic pressure
$\bar{p}$ = time-mean hydrodynamic pressure
p' = acoustic pressure
$\mathbf{Q}$ = vector of conservative variables
r_c = core radius of the Scully vortex model
r_0 = radius of rotation of vortex pair
$\mathbf{S}, \mathbf{S}_1$ = source term in acoustic equation
T = period of rotation (spinning vortex pair)
t = time
$\mathbf{U}$ = vector of primitive variables
u, v = hydrodynamic velocity components
u', v' = acoustic velocity components
$\mathbf{X}, \mathbf{Y}$ = eigen-vector matrix of $\mathbf{A}$ and $\mathbf{B}$
x, y = Cartesian coordinates
Y_2 = Bessel function of the 2^{nd} kind of order 2
Γ = Circulation (+: counterclockwise)
γ = ratio of specific heat
θ = angular argument
λ = wave length
$\Lambda, \mathbf{M}$ = diagonal matrix of $\mathbf{A}$ and $\mathbf{B}$
ξ, η = body-fitted coordinates
ρ_0 = ambient density
ρ_1 = hydrodynamic density correction
ρ' = acoustic density
σ_t = weighting factor in time stepping
ϕ = velocity potential
ω = angular velocity

*선임 연구원, 한국항공우주 연구소
†학생회원, 한국과학기술원 항공우주공학과
‡정회원, 한국과학기술원 항공우주공학과

1. Introduction

The motions of vorticity are considered to be directly related to the source of sound generated by vortical flows. These phenomena have been studied both theoretically [1 – 7] and numerically [8 – 19] by many researchers.

In accordance with the developments in computational fluid dynamics, computational aeroacoustics (CAA) provides a useful tool for analyzing the mechanism of aeroacoustic sound generation and propagation. There are several approaches in CAA to calculate the sound field. Lele [8], Colonius *et al.* [9], Mitchell *et al.* [10], and Tam and Webb [11] have obtained results by direct simulation of Navier-Stokes equations. Direct simulation of Navier-Stokes equations is the most desirable method, but it requires a higher order numerical scheme. Huh *et al.* [12] and Watson and Myers [13] solved the perturbed acoustic equations derived from the Euler equations to calculate propagation, scattering, or diffraction of incoming waves. However, the perturbed Euler equations cannot predict the sound generated by inherent unsteadiness of the flow because of the homogeneity of the equations.

Hardin and Pope [14, 15] proposed a computational aeroacoustics technique, where they split the Euler equations into hydrodynamic terms and perturbed acoustic terms. The novelty of their approach is found in the introduction of a new variable named 'hydrodynamic density fluctuations', which is the basic difference in the formulation of governing equations from others [12, 13]. They applied the technique to the problems of a pulsating and an oscillating sphere, which were acting as a monopole or a dipole source with sound-generating body surfaces.

Based on the hydrodynamic density fluctuations, we numerically studied the sound generation by quadrupole sources. The acoustic field induced by a spinning vortex pair is calculated because it has analytic solutions and represents the basic acoustic field generated by turbulent shear flows, jet flows, edge tones, etc. [5]. It is verified that the acoustic field calculated numerically agrees well with the analytical one obtained by matched asymptotic expansion (MAE). The advantage of this approach is that a conventional numerical scheme can be used to calculate the acoustic field.

In this paper, we are interested in the effect of a wall on the acoustic field generated by spinning vortices. This flow represents the basic model of the acoustic field generated by turbulent shear flows from the wall boundary layer. In the boundary layer, some coherent motions exist near the wall. These coherent motions affect the unsteady pressure fluctuations near the wall. The unsteady pressure fluctuations are strongly related to the near field sound, and parts of those energies are radiated to the far field acoustic energy. We would like to simulate near and far acoustic fields simultaneously.

2. Governing Equations

To derive the two-dimensional acoustic equations from the compressible flow governing equations, let us split the velocity, pressure and density terms into hydrodynamic terms and fluctuation terms respectively as belows:

$$\begin{aligned} \tilde{u} &= u + u' \\ \tilde{v} &= v + v' \\ \tilde{p} &= p + p' \\ \tilde{\rho} &= \rho_0 + \rho_1 + \rho' \end{aligned} \tag{1}$$

where ρ', u', v' and p' are unknown perturbed compressible acoustic density, velocities and pressure respectively; and the variables of u, v, and p are known incompressible hydrodynamic solutions of time-dependent velocity components, and pressure, respectively. The variable ρ_1 is the key parameter, which relates the incompressible hydrodynamic flow field as the sound source to the compressible acoustic filed. The parameter ρ_1, defined as the 'hydrodynamic density', is the density fluctuation induced by the hydrodynamic pressure fluctuation in the flow field. The quantity is defined by the isentropic relation as [15]:

$$\rho_1 = \frac{1}{a_0^2}(p - \bar{p}) \tag{2}$$

where

$$\bar{p} = \lim_{T\to\infty} \frac{1}{T} \int_0^T p dt$$

The hydrodynamic pressure p is obtained by the unsteady Bernoulli equation as:

$$p = p_0 - \rho_0 \frac{\partial \phi}{\partial t} - \frac{1}{2}\rho_0 (u^2 + v^2) \qquad (3)$$

where ρ_0 and p_0 are the constant quantities in the flow field.

From the above relations, the perturbed acoustic equations derived from the Euler equations for two-dimensional acoustic fields induced by unsteady, inviscid flow can be expressed in a non-dimensional generalized curvilinear coordinates form as:

$$\frac{\partial \mathbf{Q}}{\partial t} + \frac{\partial \mathbf{E}}{\partial \xi} + \frac{\partial \mathbf{F}}{\partial \eta} = -\mathbf{S} \qquad (4)$$

where

$$\mathbf{Q} = J^{-1} \begin{bmatrix} \rho' \\ \hat{\rho}u' + \rho' u \\ \hat{\rho}v' + \rho' v \end{bmatrix}$$

$$\mathbf{E} = J^{-1} \begin{bmatrix} \hat{\rho}U' + \rho' U \\ \hat{\rho}(uU' + u'U) + \rho' uU + p'\xi_x \\ \hat{\rho}(vU' + v'U) + \rho' vU + p'\xi_y \end{bmatrix}$$

$$\mathbf{F} = J^{-1} \begin{bmatrix} \hat{\rho}V' + \rho' V \\ \hat{\rho}(uV' + u'V) + \rho' uV + p'\eta_x \\ \hat{\rho}(vV' + v'V) + \rho' vV + p'\eta_y \end{bmatrix}$$

$$\mathbf{S} = J^{-1} \begin{bmatrix} \frac{\partial}{\partial t}(\rho_1) + \frac{\partial}{\partial \xi}(\rho_1 U) + \frac{\partial}{\partial \eta}(\rho_1 V) \\ \frac{\partial}{\partial t}(\rho_1 u) + \frac{\partial}{\partial \xi}(\rho_1 uU) + \frac{\partial}{\partial \eta}(\rho_1 uV) \\ \frac{\partial}{\partial t}(\rho_1 v) + \frac{\partial}{\partial \xi}(\rho_1 vU) + \frac{\partial}{\partial \eta}(\rho_1 vV) \end{bmatrix}$$

$$\hat{\rho} = 1 + \rho_1 + \rho'$$
$$J = 1/(x_\xi y_\eta - y_\xi x_\eta)$$

and

$$U = \xi_x u + \xi_y v$$
$$V = \eta_x u + \eta_y v$$
$$U' = \xi_x u' + \xi_y v'$$
$$V' = \eta_x u' + \eta_y v'$$

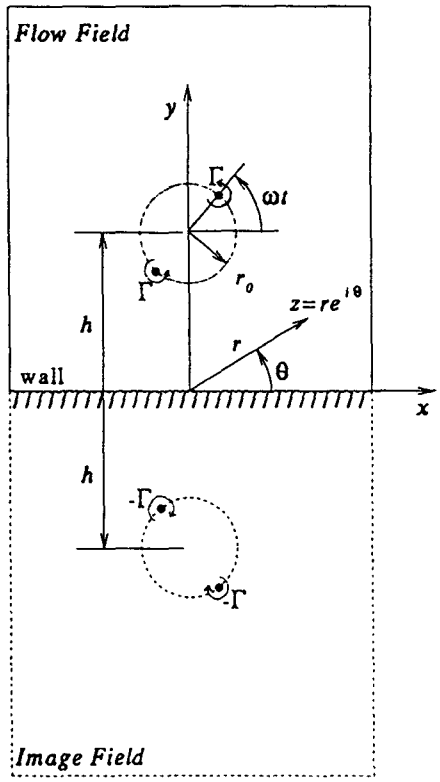

Fig. 1 Spinning vortex pair on a flat wall and its image.

The density, velocity and pressure variables in Eq. (1) are non-dimensionalized by ρ_0, a_0 and $\rho_0 a_0^2$, respectively [16,17]. The length and time variables in Eq. (4) are non-dimensionalized by r_0 and r_0/a_0 respectively. From the isentropic relation, the pressure fluctuation can be represented as below:

$$p' = \frac{1}{\gamma}(1 + \rho_1 + \rho')^\gamma - p \qquad (5)$$

3. Description of the Flow Field

The flow fields are simplified as an unsteady two-dimensional spinning vortex pair near the flat wall. The flow field can be assumed as a potential flow. The effect of the wall is represented by the mirror image method. Fig.

1 represents the schematic view of the spinning vortex pair on the flat wall with its image. The two point vortices, separated by a distance of $2r_0$ with circulation Γ, has a period $T = 8\pi^2 r_o^2/\Gamma$, rotation speed $\omega = \Gamma/(4\pi r_0^2)$, wave length $\lambda = \pi a_0/\omega$, and rotating Mach number $M_r = \Gamma/(4\pi r_0 a_0)$. In this study, the center of the vortex pair is assumed to be fixed and the vortex pair rotates in a circular motion with radius r_0 in the flow field.

In the numerical analysis for the acoustic field due to spinning vortices, a vortex core model is required to avoid the singularity at the center of the vortex. We use the Scully vortex model [21] as below:

$$V_\theta = \frac{\Gamma r}{2\pi(r_c^2 + r^2)} \tag{6}$$

where V_θ is the tangential velocity, r is a radial distance from the vortex center, and r_c is the core radius. The Scully vortex model has smoother velocity distribution than the Rankine vortex model.

4. Boundary Conditions and Scheme

Boundary conditions are very important for acoustic problems. We used the non-reflecting boundary conditions based on the impedence condition on the free field boundary to account for the oblique wave on the free boundary. Thompson's technique [20] for a generalized coordinates system is used to obtain the density fluctuation.

First, to apply the boundary conditions, Eq. (4) is linearized and recast in the following form:

$$\mathbf{Q}_1 \frac{\partial \mathbf{U}}{\partial t} + \mathbf{E}_1 \frac{\partial \mathbf{U}}{\partial \xi} + \mathbf{F}_1 \frac{\partial \mathbf{U}}{\partial \eta} = -\mathbf{S} \tag{7}$$

where

$$\mathbf{U} = [\rho', u', v']^T$$

$$\mathbf{Q}_1 = \frac{\partial \mathbf{Q}}{\partial \mathbf{U}}, \quad \mathbf{E}_1 = \frac{\partial \mathbf{E}}{\partial \mathbf{U}}, \quad \mathbf{F}_1 = \frac{\partial \mathbf{F}}{\partial \mathbf{U}}$$

or

$$\frac{\partial \mathbf{U}}{\partial t} + \mathbf{A}\frac{\partial \mathbf{U}}{\partial \xi} + \mathbf{B}\frac{\partial \mathbf{U}}{\partial \eta} = -\mathbf{S}_1 \tag{8}$$

where

$$\mathbf{A} = \mathbf{Q}_1^{-1}\mathbf{E}_1, \quad \mathbf{B} = \mathbf{Q}_1^{-1}\mathbf{F}_1, \quad \mathbf{S}_1 = \mathbf{Q}_1^{-1}\mathbf{S}$$

Matrices $\mathbf{A}$ and $\mathbf{B}$ can be diagonalized by the similarity transformations.

$$\mathbf{X}\mathbf{A}\mathbf{X}^{-1} = \Lambda, \quad \mathbf{Y}\mathbf{B}\mathbf{Y}^{-1} = \mathbf{M}$$

where the diagonal elements of Λ and $\mathbf{M}$ are the eigen values of $\mathbf{A}$ and $\mathbf{B}$ and can easily be obtained as:

$$\Lambda = \mathrm{diag}\left(U - \sqrt{\xi_x^2 + \xi_y^2}, U, U + \sqrt{\xi_x^2 + \xi_y^2}\right)$$

$$\mathbf{M} = \mathrm{diag}\left(V - \sqrt{\eta_x^2 + \eta_y^2}, V, V + \sqrt{\eta_x^2 + \eta_y^2}\right)$$

Thompson's boundary conditions [20], however, have the limitation of not reproducing the outgoing acoustic signals except for planar waves. To compensate for this limitation, additional physical boundary conditions are considered here. The basic concept is that the acoustic wave radiating through the far boundary is thought to be a cylindrical plane wave. This physical condition with an isentropic assumption gives the relations [17]:

$$p' = u'_{\text{radial}} = \rho' \tag{9}$$

In the above modified boundary conditions, only p' is calculated from Thompson's non-reflecting boundary condition, and the remaining two components are evaluated from above equation.

The acoustic boundary condition on the rigid wall is similar to the flow boundary condition as belows:

$$V = 0, \quad V' = 0, \quad \frac{\partial \rho'}{\partial \eta} = 0, \quad \frac{\partial p'}{\partial \eta} = 0 \tag{10}$$

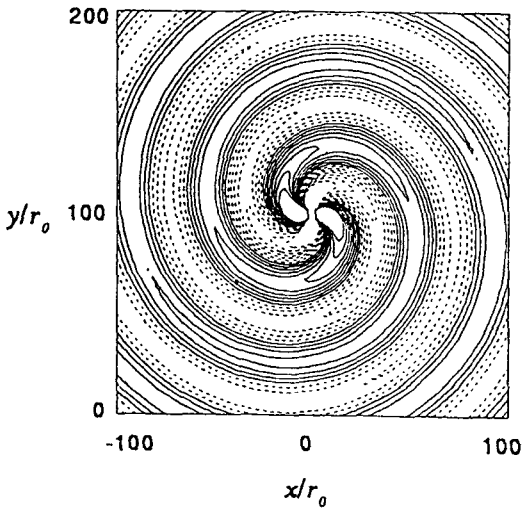

Fig. 2 Analytical acoustic pressure contour of the spinning vortex pair for $\Gamma/a_0 r_0 = 1$, $M_r = 0.0796$ in the free field, $(-2.5E-4 < p' < 2.5E-4$, 16-steps).

MacCormack's predictor-corrector scheme has gained wide use and acceptance for solving time-dependent problems in fluid dynamics [22] and is used in the present study to integrate both the interior and the boundary points of Eq. (4). The time-step to meet the Courant-Friedrichs-Lewy (CFL) criterion is determined according to:

$$\Delta t = \sigma_t / \Delta t_c \tag{11}$$

where

$$\Delta t_c = \left[\frac{|U|}{\Delta\xi} + \frac{|V|}{\Delta\eta} + a_0 \sqrt{\frac{\xi_x}{\Delta\xi^2} + \frac{\eta_y}{\Delta\eta^2}} \right]$$

and σ_t is a positive constant less than 1. In this study, we used $\sigma_t = 0.9$ for the flat wall and 0.6 for the circular cylinder problem.

5. Results and discussions

5.1. Verification

From the MAE, the theoretical solution for the spinning vortex pair in the free field can easily be obtained. In the MAE method, the solutions of the equations for incompressible motion in the flow domain and a homogeneous compressible wave equation in the acoustic field are matched in an intermediate domain in such a way as to give an asymptotically valid solution. From the MAE, the amplitude of the pressure fluctuation for the spinning vortex pair in the free field can be represented as below [2], [18]:

$$p'(r,\theta,t) = -\frac{\Gamma \rho_0 \omega k^2 r_0^2}{4} \big(J_2(kr) \sin 2(\theta - \omega t) + Y_2(kr) \cos 2(\theta - \omega t) \big) \tag{12}$$

The pressure contour of above equation is shown in Fig. 2 for $\Gamma/a_0 r_0 = 1$, $M_r = 0.0796$ at time $t = 10T$, which results in the typical acoustic pattern of the quadrupole acoustic source in the free field. The acoustic pressures on the two far boundary lines are shown in Fig. 3.

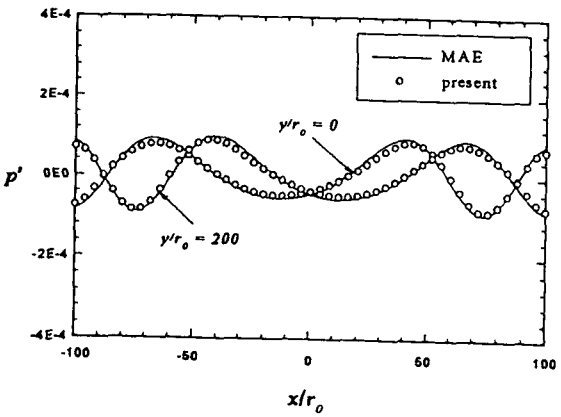

Fig. 3 Acoustic pressures on the boundary lines, $y/r_0 = 0$ and $y/r_0 = 200$, for the spinning vortex pair in the free field (no rigid wall boundaries) for $\Gamma/a_0 r_0 = 1$, $M_r = 0.0796$ at time $t = 10T$.

The numerical boundary conditions in Eq. (10) are compared with the image method by calculating the spinning vortex on a flat plane as shown in Fig. 1. Fig. 4 shows the acoustic pressure distributions for $y/r_0 = 60$ and $y/r_0 = 140$. In this figure, we compared the result of the numerical wall boundary conditions

with the result obtained by using the acoustic image method for verification of the boundary conditions.

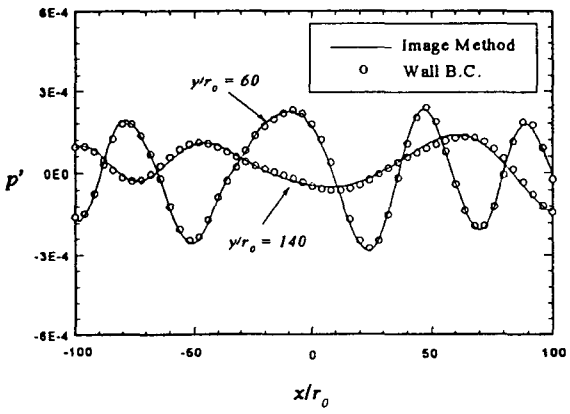

Fig. 4 Comparison of acoustic pressure distribution along the $y/r_0 = 60, 140$ lines for $\Gamma/a_0 r_0 = 1$, $M_r = 0.0796$ at time $t = 10T$.

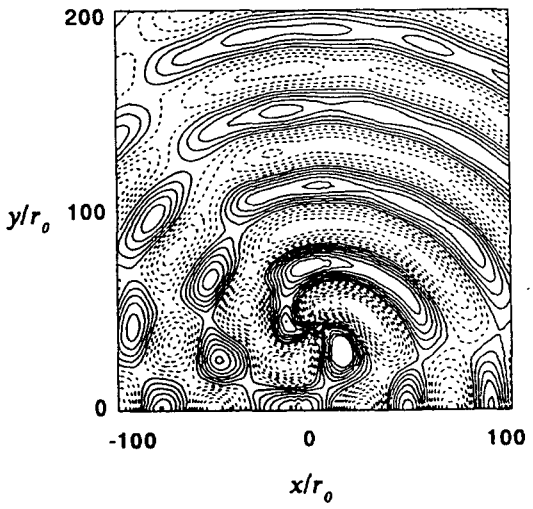

Fig. 5*a* Acoustic pressure contour for $\Gamma/a_0 r_0 = 1$, $M_r = 0.0796$, $h/r_0 = 40$ at time $t = 10T$. The dashed line is negative value ($-2.5E-4 < p' < 2.5E-4$, 16-steps).

5.2. Flat wall effects

The computational domain has rectangular dimensions of $(L/r_0 \times L/r_0) = (200 \times 200)$ and grid system of 101×101. The spinning vortex is assumed to start abruptly at time $t = 0$. Analytical solutions of the hydrodynamic flow field are evaluated at each time-step over the computational domain and are used as the source term in Eq. (7). The rigid wall is located at $y/r_0 = 0$ as shown in Fig. 1, and the acoustic boundary conditions are shown in Eq. (10); that is, rigid wall boundary conditions.

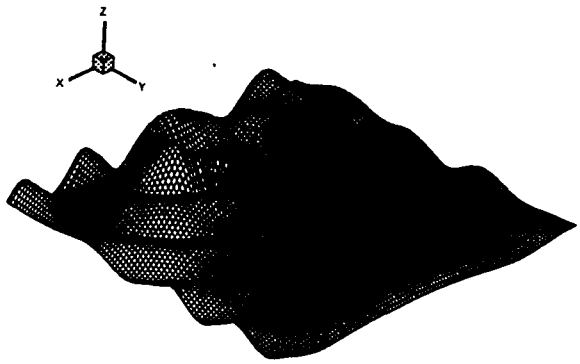

Fig. 5*b* Three-dimensional graphical view of acoustic pressure for $\Gamma/a_0 r_0 = 1$, $M_r = 0.0796$, $h/r_0 = 40$ at time $t = 10T$. The upper-left side is wall boundary (z-direction represents the magnitude of $p' \times 200$).

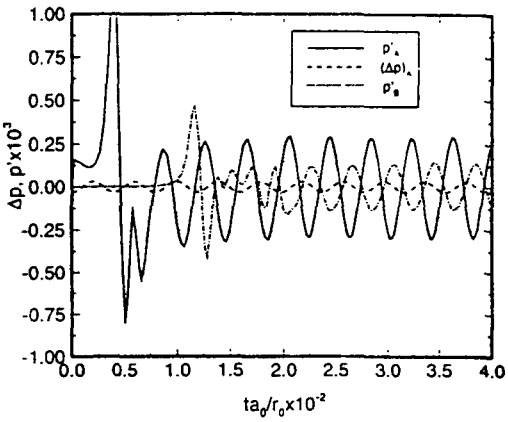

Fig. 5c Comparison of acoustic pressure and wall pressure variation at the field point A, B according to time (point A: $(x/r_0, y/r_0) = (0, 0)$, point B:

$(x/r_0, y/r_0) = (100, 100))$ for $\Gamma/a_0 r_0 = 1$, $M_r = 0.0796$, $h/r_0 = 40$ at time $t = 10T$.

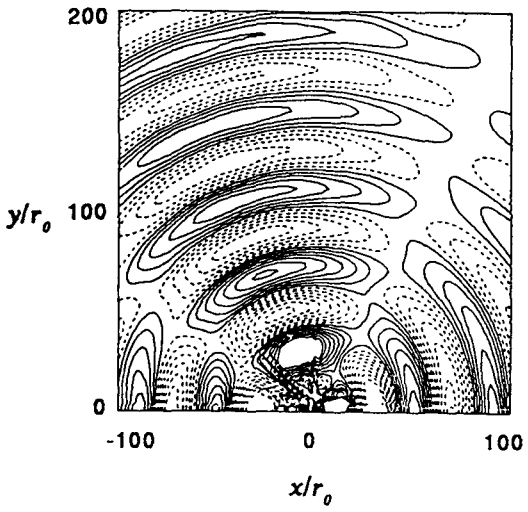

Fig. 6*a* Acoustic pressure contour for $\Gamma/a_0 r_0 = 1$, $M_r = 0.0796$, $h/r_0 = 4$ at time $t = 10T$. The dashed line is negative value $(-2.5E-4 < p' < 2.5E-4$, 16-steps).

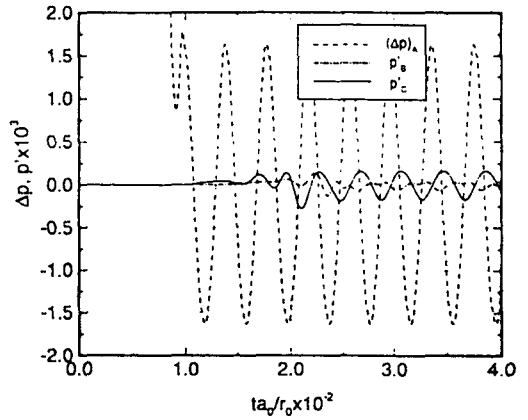

Fig. 6*b* Comparison of acoustic pressures and wall pressure variation at the field point A, B and C according to time (point A: $(x/r_0, y/r_0) = (0, 0)$, point B: $(x/r_0, y/r_0) = (100, 100)$, and point C: $(x/r_0, y/r_0) = (0, 104)$ which has $100r_0$ above the source) for $\Gamma/a_0 r_0 = 1$, $M_r = 0.0796$, $h/r_0 = 4$ at time $t = 10T$.

Fig. 5*a* represents the acoustic pressure contours for a case of $\Gamma/a_0 r_0 = 1$, $M_r = 0.0796$, $h/r_0 = 40$. In this case, the distance from the wall to the acoustic source is nearly $1\lambda(\lambda/r_0 = 39.47)$. The three-dimensional graphical view is represented in Fig. 5*b*. From Fig. 5*a*, we can observe the interaction phenomena between the waves from the spinning vortex pair and the reflecting waves from the rigid flat wall. We can observed that the acoustic waves are radiated from around $(x, y) = (0, 0)$ to the far field. Three series of wave propagating modes on the left field, one series of them on the midfield, and one series of them on the right field can be observed. Unlike the spinning vortex in the free field as shown in Fig. 2, the results represent an asymmetric directivity pattern. In Fig. 5*a*, the waves are generated from the spinning vortex pair, and propagated toward the wall. The incident wave angles on the left wall are greater than those on the right wall. When the incident angle is zero (grazing wave), no reflecting waves are generated from the wall. The more growing the incident angle, the more growing the interfering region. For this reason, wave interference of the left field by the reflection wave becomes more severe than that of the right field. These phenomena break the symmetric directivity pattern of the spinning quadrupole source.

Fig. 5*c* represents the hydrodynamic pressure fluctuation and acoustic pressure variations on the wall (point A) and acoustic pressure variation in the field (point B) according to the non-dimensional time (point A: $(x/r_0, y/r_0) = (0, 0)$, point B: $(x/r_0, y/r_0) = (100, 100)$).

Fig. 6*a* represents the acoustic pressure contours for a case of $\Gamma/a_0 r_0 = 1$, $M_r = 0.0796$, $h/r_0 = 4$ which can be compared with the result of Fig. 5*a*. The distance from the wall to the acoustic source is nearly 0.1λ. We can observe different series of acoustic peaks in left and right fields. Fig. 6*b* represents the hydrodynamic pressure fluctuation and acoustic pressure variations on the wall (point A) and acoustic pressure variation in the field (point B) according to non-dimensional time (point

A: $(x/r_0, y/r_0) = (0, 0)$, point B: $(x/r_0, y/r_0) = (100, 100)$, and point C: $(x/r_0, y/r_0) = (0, 104)$ which has $100r_0$ above the source).

From Fig. 5*c*, the hydrodynamic pressure fluctuation is not larger than the acoustic pressure fluctuation at the wall (point A). In Fig. 6*b*, however, the hydrodynamic pressure fluctuation has a larger value than acoustic pressure fluctuation at that point. In spite of this main difference, we can find that the effect of acoustic source separation from the wall does not severely affect acoustic pressure fluctuation at the far field.

6. Conclusion

A computational aeroacoustic technique, which splits Euler equations into hydrodynamic terms and perturbed acoustic terms, is applied to the case of a spinning vortex pair near a flat wall. It is found that the sound generated by the unsteady vortical flows in the presence of a body surface can be calculated by using the source terms due to the hydrodynamic pressure fluctuations. The spinning vortex pair in a free field generates a typical quadrupole directivity pattern, whereas for the spinning vortex pair near the wall, the acoustic directivity patterns show a scattering acoustic field due to the wall. From the above reason, a more silent zone can exist in the near field region as compared with the far field. It will be possible for the perturbed Euler equations based on the hydrodynamic density to predict more complex acoustic fields when the flow information is obtained.

References

[1] Powell, A., "Theory of Vortex Sound," *Journal of the Acoustical Society of America*, Vol. 36, No. 1, (1964), pp. 177-195

[2] Müller, E.A., and Obermeier, F., "The Spinning Vortices as a Source of Sound," AGARD CP-22, (1967), pp. 22.1-22.8

[3] Howe, M.S., "Contribution to the Theory of Aerodynamic Sound, with Application to excess Jet Noise and the Theory of the Flute," *Journal of Fluid Mechanics*, Vol. 71, (1975), pp. 625-673

[4] Obermeier, F., "The Application of Singular Perturbations Methods to Aerodynamic Sound Generation," *Singular Perturbations and Boundary Layer Theory*, edited by Brouner, Gray and Mathieu, Springer-Verlag, Berlin, (1977), pp. 401-421

[5] Yates, J.E., "Application of the Bernoulli Enthalpy Concept to the Study of Vortex Noise and Jet Impingement Noise," NASA CR2987, (1978)

[6] Möhring, W., "On Vortex Sound at Low Mach Number," *Journal of Fluid Mechanics*, Vol. 85, (1978), pp. 685-691

[7] Kambe, T., "Acoustic Emissions by Vortex Motions," *Journal of Fluid Mechanics*, Vol. 173, (1986), pp. 643-666.

[8] Lele, S.K., "Direct Numerical Simulation of Compressible Free Shear Flows," AIAA Paper 89-0374, Jan. (1989)

[9] Colonius, T., Lele, S.K., and Moin, P., "Scattering of Sound Waves by a Compressible Vortex," AIAA Paper 91-0494, (1991)

[10] Mitchell, B.E., Lele, S.K., and Moin, P., "Direct Computation of the Sound from a Compressible Co-rotating Vortex Pair," AIAA Paper 92-0374, (1992)

[11] Tam, C.K.W., and Webb, J.C., "Dispersion-Relation-Preserving Schemes for Computational Acoustics," DGLR/AIAA 92-02-033, May (1992)

[12] Huh, K.S., Agrawal, R.K., and Widnall, S. E., Numerical Simulation of Acoustic Diffraction of Two-dimensional Rigid Bodies in Arbitrary Flows," AIAA Paper 90-3920, (1990)

[13] Watson, W.R., and Myers, M.K., "A Two-step Method for Evolving Acoustic Systems to a Steady-state," AIAA Paper 90-3946, (1990)

[14] Hardin, J.C., and Pope, D.S., "Sound Generated by a Stenosis in a Pipe," AIAA Paper 90-3919, (1990)

[15] Hardin, J. C., and Pope, D.S., "A New Technique for Aerodynamic Noise Calculation," DGLR/AIAA 92-02-076, (1992)

[16] Lee, D.J. and Koo, S.O., "Numerical Study of Sound Generation Due to a Spinning Vortex Pair," *AIAA Journal* Vol. 33, No. 1, (1995), pp. 20-26

[17] Koo, S.O., "Numerical Study of Acoustic Fields Generated by Unsteady Vortical Flows," Ph.D. Thesis, KAIST, (1995)

[18] Koo, S.O., Ryu, K.W., and Lee, D.J., "Calculation of Near and Far Acoustic Fields Due to a Spinning Vortex Pair in Free Field," Journal of Computational Fluids Engineering, (1997)

[19] Ryu, K.W., and Lee, D.J., and Koo, S.O., "Sound Generation Due to a Spinning Vortex Pair Near the Flat and Curved Wall," AIAA Paper 96-1748, (1996)

[20] Thompson, K.W., "Time Dependent Boundary Conditions for Hyperbolic Systems," *Journal of Computational Physics*, Vol. 68, (1987), pp. 1-24

[21] Scully, M.P., "Computational of helicopter Rotor Wake Geometry and Its Influence on Rotor Harmonic Airloads," MIT, Pub. ARSL TR 178-1, Cambridge, MA, March, (1975)

[22] Anderson, D.A., Tannehill, J.C., and Pletcher, R.H., *Computational Fluid Mechanics and Heat Transfer*, McGraw-Hill, New York, (1984)